BYL719, a new α-specific PI3K inhibitor: Single administration and in combination with conventional chemotherapy for the treatment of osteosarcoma

Bérengère Gobin, Marc Baud' Huin, François Lamoureux, Benjamin Ory, Céline Charrier, Rachel Lanel, Séverine Battaglia, Françoise Rédini, Frédéric Lézot, Frédéric Blanchard, et al.

BYL719, a new α-specific PI3K inhibitor: single administration and in combination with conventional chemotherapy for the treatment of osteosarcoma

Bérengère GOBIN[1,2], Marc BAUD'HUIN[1,2], François LAMOUREUX [1,2], Benjamin ORY[1,2], Céline CHARRIER[1,2,3], Rachel LANEL[1,2], Séverine BATTAGLIA[1,2], Françoise REDINI[1,2,3,4], Frédéric LEZOT[1,2], Frédéric BLANCHARD[1,2,3] and Dominique HEYMANN[1,2,3,4]

[1]INSERM, UMR 957, Nantes F-44035, France
[2]Université de Nantes, Physiopathologie de la Résorption Osseuse et Thérapie des Tumeurs Osseuses Primitives, Nantes F-44035, France
[3]Equipe LIGUE Nationale Contre le Cancer 2012, Nantes F-44035, France
[4]CHU de Nantes, Nantes F-44035, France

Novelty & Impact Statements: Targeting PI3Kα using a novel inhibitor, BYL719 decreases cell proliferation by blocking cell cycle in G0/G1 phase and inhibits cell migration, but fails to induce cell death in osteosarcoma cells. In addition, BYL719 exhibits dual activities on osteoblast and osteoclast differentiation. We specifically report, in murine pre-clinical models of osteosarcoma, BYL719 monotherapy significantly reduces the tumor progression, tumor ectopic bone formation and tumor vascularization. Importantly, the combination of BYL719 with ifosfamide shows promising efficacy.

Running title: BYL719 PI3Kα inhibitor: therapeutic value in osteosarcoma

Key words: osteosarcoma, osteoblast, osteoclast, vascularization, PI3K, mTOR

***Corresponding author:**
Prof. Dominique Heymann
INSERM UMR 957
Faculty of Medicine, 1 rue Gaston Veil
44035 Nantes cedex, France
Phone: 33 (0) 272 641 132;Fax : 33 (0) 240 412 860

E-mail: dominique.heymann@univ-nantes.fr

ABSTRACT

It has been established that disturbances in intracellular signaling pathways play a considerable part in the oncologic process. Phosphatidylinositol-3-kinase (PI3K) has become of key interest in cancer therapy because of its high mutation frequency and/or gain in function of its catalytic subunits in cancer cells. We investigated the therapeutic value of BYL719, a new specific PI3Kα inhibitor that blocks the ATP site, on osteosarcoma and bone cells. The *in vitro* effects of BYL719 on proliferation, apoptosis and cell cycle were assessed in human and murine osteosarcoma cell. Its impact on bone cells was determined using human mesenchymal stem cells (hMSC) and human $CD14^+$ osteoclast precursors. Two different murine preclinical models of osteosarcoma were used to analyze the *in vivo* biological activities of BYL719. BYL719 decreased cell proliferation by blocking cell cycle in G0/G1 phase with no outstanding effects on apoptosis cell death in HOS and MOS-J tumor cells. BYL719 inhibited cell migration and can thus be considered as a cytostatic drug for osteosarcoma. In murine pre-clinical models of osteosarcoma, BYL719 significantly decreased tumor progression and tumor ectopic bone formation as shown by a decrease of $Ki67^+$ cells and tumor vascularization. To explore the maximum therapeutic potential of BYL719, the drug was studied in combination with conventional chemotherapeutic drugs, revealing promising efficacy with ifosfamide. BYL719 also exhibited dual activities on osteoblast and osteoclast differentiation. Overall, the present work shows that BYL719 is a promising drug in either a single or multi-drug approach to curing bone sarcoma.

INTRODUCTION

Osteosarcoma is the most common form of primary malignant bone tumor, diagnosed in children and young adults. The survival rate reaches approximately 50% to 70 % at 5 years for patients with a localized pathology but drops to 30 % when pulmonary metastases are detected at diagnosis (1,2). Unfortunately, these levels have remained unchanged in the last few decades (3-5) and consequently the lack of response to conventional treatment in many patients with osteosarcoma shows the urgency for developing new therapies. The most up-to-date knowledge on the biology of bone sarcomas has led to the identification of new therapeutic targets expressed by tumor cells and/or their microenvironment (3-7). Cancer cell proliferation, apoptosis and drug resistance are frequently mediated by a very complex network of intracellular signaling pathways and identify various potential targets. In this context, the proteins mediating kinase activities have been targeted by monoclonal antibodies directed against extra-membranous receptors or by small chemical inhibitors.

Of these protein kinases, the PhosphoInositol-3-Kinase (PI3K) pathway regulates numerous basic biological processes (cell cycle; cell proliferation; survival and migration, etc) (7-11). Class I PI3Ks are heterodimers composed of one catalytic subunit (p110) and one regulatory subunit (p85-like subunit for Class Ia; p101 or p84 for Class Ib) (12). Class I PI3Ks are key partners in cell signaling initiated by the activation of the receptor tyrosine kinase (RTK), G protein-coupled receptors or from activated RAS. In many forms of cancer, such as in breast, prostate or lung cancer, this key pathway is frequently dysregulated and associated with a gain in mutation function and/or amplification of the *PIKCA* gene, loss of *PTEN* expression, and amplification/overexpression of RTK or AKT mutations (13,14). PI3Ks are involved in the proliferation and migration of osteosarcoma cells, and also in an anti-apoptotic

effect or in drug responses/resistance (15-20). Three mutations of *PIK3CA* (H1047R, E545K, and H701P) have recently been described for the first time in a series of 89 osteosarcomas (incidence: 3.3 %). Two of the 3 samples with PIK3CA mutations were associated with active AKT signaling pathway (detectable pAKT) and all 3 samples showed detectable p4EBP1 (21). Based on these observations, it would be interesting to evaluate the efficacy of PI3K inhibitors. Thus, several pan-, dual- or specific PI3K inhibitors have been developed, assessed in pre-clinical models and in clinical trials including patients suffering from various solid tumors (breast carcinoma, bladder carcinoma, melanoma, etc) (14).

BYL719 is a new α-specific PI3K inhibitor developed on the basis of a binding model (22), and tested in clinical trials in patients with advanced solid malignancies carrying the PIK3CA alteration (23,24). BYL719 thus appears to be a promising agent for the treatment of neoplastic diseases. Consequently, the aim of the present study was to investigate the therapeutic value of BYL719 in osteosarcoma, alone or in combination with conventional chemotherapy. We also investigated the effects of this new PI3K inhibitor on bone cells and bone remodeling.

MATERIALS AND METHODS

Cell lines and culture conditions

Human osteosarcoma MG-63 and HOS-MNNG (HOS) cells purchased from the ATCC (USA) and rat osteosarcoma OSRGA cell line (25, 26) were cultured in DMEM (Lonza, Belgium) supplemented with 5% of Fetal Bovine Serum (FBS; Hyclone Perbio, France). Murine osteosarcoma POS-1 (27) and MOS-J (28) cells were cultured in RPMI (Lonza) supplemented with 5% of FBS.

Cell growth and viability, clonogenic assay

Two thousand tumor cells were seeded into 96-well plates and, the day after, the cells were treated with BYL719 (1 to50 µmol/L) provided by Pharma Novartis (Basle, Switzerland) for 72 hours. Cell growth/viability were determined using a colorimetric assay using sodium 3'[1-(phenylaminocarbonyl)-3,4-tetrazolium]-bis(4-methoxy-6-nitro-)benzene sulfonic acid hydrate (XTT reagent assay kit; Roche Molecular Biochemicals, Germany). Absorbance was read at 490nm. Cell viability was also determined by trypan blue exclusion assay; viable and non-viable cells were counted manually after 24 and 48 hours of treatment. For clonogenic assay, tumor cells were pre-treated with or without 25 µM BYL for 6h following by treatment with/without 5 µg/ml Mafosfamide for 48h in 96-well plate. Then, the tumor cells were splitted in 6-wells plate, with 500 cells/well without treatment for 7 days. The number of colonies was counted after crystal violet staining.

The combination index (CI) was evaluated using CalcuSyn dose effect analysis software (Biosoft, Cambridge, UK). This method, based on the multiple drug effect equation of Chou-Talalay, is suitable for calculating combined drug activity over a wide range of growth

inhibition: CI =1, additivity; CI >1, antagonism; CI <1, synergism. CI was calculated at ED_{50}, ED_{75} and ED_{90}.

Caspase activity

Two hundred thousand cells were seeded in 6-well plates and cultured with or without BYL719 for 3 to 48 hours (25 μM). Caspase activity was assessed using the CaspACE Assay System kit (Promega), according to the manufacturer's recommendations. Results were expressed in arbitrary units, corrected for protein concentration quantified by BCA (Sigma). Cell lysate of cells treated with 1μg/ml of Staurosporine (Invitrogen) over-night was used as the positive control.

Cell cycle analysis

Subconfluent cultures were incubated with or without 25 μM of BYL719 for 18 hours, trypsinized, washed and incubated in PBS containing 0.12% Triton X-100, 0.12 mM EDTA and 100 μg/ml DNase-free ribonuclease A (Sigma). Then, 50 μg/ml of propidium iodide (Promega) were added for 20 minutes. Cell cycle distribution was determined by flow cytometry (Cytomics FC500; Beckman Coulter) and analyzed by DNA cell Cycle Analysis Software (Phoenix Flow System, USA).

Western blots

Two hundred thousand cells were treated with 25 μM of BYL719 for 3 to 24 hours and then lysed in RIPA buffer (150 mmol/L NaCl, 5% Tris, pH 7.4, 1% NP-40, 0.25% sodium deoxycholate, 1mmol/L Na_3VO_4, 0.5 mmol/L PMSF, 10 mg/mL leupeptin, 10 mg/mL aprotinin). Total cell lysate (40 μg), determined using the BCA kit, was run on 10% SDS-PAGE and electrophoretically transferred to Immobilon-P membranes (Millipore). The

membrane was blotted with antibodies (Supplementary Data 1) in PBS, 0.05% Tween 20, and 3% BSA. Antibody binding was visualized using the enhanced chemiluminescence system (Roche Molecular Biomedicals).

Osteoblast differentiation

Peripheral blood and bone marrow, harvested by iliac crest aspiration from healthy donors was obtained from the "Etablissement Français du Sang" (Nantes, France) with informed consent and ethical approval. Human mesenchymal stem cells (hMSC) were cultured in DMEM supplemented with 10% of FBS, 1 ng/ml of basic Fibroblast Growth Factor (bFGF; R&D systems, UK), 100 U/ml of penicillin/streptomycin, and 2 mM L-glutamine. Adherent cells were frozen at passage 2 after characterization by flow cytometry ($CD45^-$, $CD34^-$, $CD105^+$, $CD73^+$, and $CD90^+$, purity ≥99%) prior to further experiments (29,30). Two hundred thousand hMSCs were seeded in 24-well plates in proliferation medium and allowed to attach and reach confluence (this represented day 0 for hMSC osteogenic differentiation). After 3 days, the medium was changed without bFGF but supplemented with vitamin D3 (10^{-8} M; Sigma, France) and dexamethasone (10^{-7} M; Sigma), with or without BYL719. Three days later, ascorbic acid (50 ng/ml; Sigma) and b-glycerophosphate (10 mM; Sigma) were added to allow mineralization detected by alizarin red-S staining as described previously (30,31). Images were captured using a stereomicroscope (Stemi 2000-C; Zeiss), and mineralized surfaces were quantified using Qwin software (Leica, Germany).

Osteoclastogenesis assay

$CD14^+$ cells (purity around 96%) were isolated from human peripheral blood, using MACS microbeads (Miltenyi Biotec, Germany) as previously described (32,33). α-MEM (Lonza) containing 10% FCS, 25ng/ml human Macrophage Colony Stimulating Factor (hM-CSF; R&D

Systems) and 100ng/mL human Receptor Activator of Nuclear Factor KappaB Ligand (hRANKL; R&D Systems) were changed every 3 days. After 11 days of culture for the $CD14^+$ cells, osteoclasts were visualized by means of TRAP staining (Sigma). To study the effect of BYL719 on osteoclast survival, hRANKL and hM-CSF were removed for 3 days after the differentiation period and $TRAP^+$ viable osteoclasts cultured with or without BYL719 were counted manually. The resorption capacity of the osteoclasts was assessed after $CD14^+$cell culture on dentine slices, with or without 25ng/mL hMCSF, 100ng/mL RANKL with or without 5µM BYL719 (33). After 11 days of culture, the adherent cells were removed manually to observe resorption pits on dentine slices by scanning electron microscopy (TM3000, Hitachi). The areas of resorption were quantified using Qwin software (Leica).

Real-time polymerase chain reaction

Total RNA was extracted using NucleoSpin® RNAII (Macherey Nagel, Germany). First-strand cDNA was synthesized from 5 µg total cell RNA with ThermoScript™ RT (Invitrogen, France) and oligo(dT) primers, according to the manufacturer's recommendations. Quantitative real-time PCR (qPCR) was carried out on a Chromo4™ System (Biorad, France) with a reaction mix containing 15-40ng reverse-transcribed total RNA, 300 nM primers (Supplementary data 2) and 2X SYBR green buffer (Biorad). The analysis was performed according to the method described by Vandesompele *et al.* (34), using GAPDH and β-actin (ACTB) as invariant controls. The data was analyzed using the DDCt method (35).

***In vivo* experiment mouse models of osteosarcoma**

The mice (Elevages Janvier, France) were housed in pathogen-free conditions at the Experimental Therapy Unit (Faculty of Medicine, Nantes) in accordance with the institutional guidelines of the French Ethical Committee and under the supervision of the authorized

investigators. The Institutional Animal Care and Use Committee (CEEA PdL 06) approved specifically the study (authorization number: 1280.01).

Syngenic model of osteoblastic osteosarcoma

Five-week-old male C57Bl/6J mice were anesthetized by inhalation of an isoflurane/air mixture (2%, 1L/min) before intramuscular injection of 1 x 10^6 mouse MOS-J osteosarcoma cells in close proximity to the tibia, leading to a rapidly growing tumor in soft tissue with secondary contiguous bone invasion. Tumors appeared at the injection site 8 days later and led to osteoblastic lesions reproducing the osteoblastic form of human osteosarcoma (20). Three groups (n=6 per group) of C57Bl/6J were assigned randomly to receive either placebo [oral administration of methylcellulose 0.5 % (Sigma)] or BYL719 (oral administration, 12.5-50 mg/kg daily). The preventive treatment started 1 day after tumor cells inoculation. Four groups of 6 C57Bl/6J were assigned randomly to receive either placebo (oral administration of methylcellulose 0.5 % and intraperitoneal injection of water), BYL719 (oral administration of 50 mg/kg/day), ifosfamide (intraperitoneal injection of 30 mg/kg 3 times during the first week), or a combination of BYL719 (50 mg/kg daily) and ifosfamide (30 mg/kg, 3 times during the first week).

Xenogenic model of osteoblastic osteosarcoma

Five-week-old female Rj:NMRI-nude mice were anesthetized as previously described before intramuscular inoculation of 2 x 10^6 human HOS-MNNG osteosarcoma cells. Tumors appeared at the injection site 8 days later and lead to osteoblastic lesions reproducing the osteoblastic form of human osteosarcoma. Two groups (n=8 per group) of mice were assigned randomly to receive either placebo (methylcellulose 0.5 %) or BYL719 (50 mg/kg daily). The preventive treatment started 1 day after tumor cells inoculation.

For both models, the tumor volumes were calculated by measuring two perpendicular diameters using calipers, according to the following formula: $V=0.5xLx(S)^2$, in which L and S

are, respectively, the largest and the smallest perpendicular diameters as previously described (20). The tumor volumes were measured twice a week until the ethical volume. The mice were sacrificed by cervical dislocation for ethical reasons when the tumor volume reached 2000 mm^3. At the end of experiment, analysis of the bone microarchitecture was performed using the high-resolution X-ray micro-computed tomography (μCT) system for small-animal imaging Sky-Scan-1076 (SkyScan, Belgium). All tibias/fibulas were scanned using the same parameters (pixel size 18 μm, 50 kV, 0.5mm alumium filter and a 0.8 degree of rotation stage). Three-dimensional reconstructions were produced using CTvox software (Skyscan). Two-dimensional analyses of bone parameters were carried out on 200 layers (cortical aera) using the CTan software (Skyscan).

Bone histology and immunohistochemistry

After euthanasia, the tibias were conserved and fixed in 10% buffered paraformaldehyde (PFA), decalcified with 13% EDTA, 0.2% PFA in PBS using a microwave tissue processor (KOS, Mikron Instruments, USA) for 5 to 7 days and embedded in paraffin. 3μm sections were cut and stained in accordance with the Masson-trichrome method (20). For TRAP staining, serial 4-μm-thick sagittal sections were prepared and stained to identify osteoclasts by 1-hour incubation in a 1 mg/mL naphthol AS-TR phosphate, 60 mM NN-dimethylformamide, 100 The stained surface was quantified using ImageJ (NIH, USA) (36). Immunohistochemistry was carried as previously described (32) using the antibodies listed in Supplementary data 1. All images were assessed by light microscopy using a DMRXA microscope (Leica, Germany). Positive immunostaining was quantified using Qwin software (Leica).

Statistical Analysis

Each experiment was repeated independently 3 times. Results were given as a mean ± standard deviation (SD) (for *in vitro* experiments) and mean ± SEM for (*in vivo* experiments) and were compared with an Unpaired t test or ANOVA test using GraphPadInStat v3.02 software. Results with $p<0.05$ were considered significant.

RESULTS

BYL719 inhibits osteosarcoma cell proliferation

As expected, Figure 1B shows that BYL719 (chemical structure in Figure 1A) rapidly inhibited the levels of P-AKT and P-mTOR in all cell lines assessed, confirming the functional activity of BYL719 on osteosarcoma cells (Figure 1B). XTT assays were then performed to analyze the effects of BYL719 on osteosarcoma cell growth (human: MG63, HOS MNNG; mouse: POS-1, MOS-J and rat: OSRGA) (Figure 1C). After 72 hours of treatment, BYL719 significantly inhibited the cell growth of all osteosarcoma cell lines tested in a dose-dependent manner (Figure 1C, D) with an IC_{50} ranging from 6 to 15 µM and with the IC_{90} from 24 to 42 µM (Figure 1E) at 72 hours. To determine whether or not the decreased cell viability induced by BYL719 was associated with a cell cycle alteration, flow cytometry of cell DNA content was performed after addition of BYL719 (Supplementary data 3). The results showed that BYL719 significantly altered the distribution of cell cycle phases and, more specifically, increased cell numbers in the G0/G1 phase from 57 to 70 % in MG-63, 44 to 73 % in HOS (Supplementary data 3A), 45 to 70 % in MOS-J and from 58 to 70 % in POS-1 cells (Supplementary data 3B). These observations were concomitant with a decrease in cells in the S-G2/M phases. Similar results were obtained on a rat osteosarcoma cell line, OSRGA (Supplementary data 4).

BYL719 acts as a cytostatic drug for osteosarcoma cells

To determine whether these effects were due to inhibition of cell proliferation and/or induction of cell death, the effects of BYL719 were assessed by manual counting of viable cells after trypan blue exclusion staining. BYL719 significantly decreases the number of alive HOS and MOS-J cells in a dose- and a time-dependent manner without affecting the number of dead cells, supporting the idea that BYL719 exerts a cytostatic activity in osteosarcoma cells (Figure 1D and Supplementary data 5A, respectively). In addition, BYL719 failed to induce apoptosis

as shown by caspase-3/7 activity assessed in HOS and MOS-J cells (Figure 1E, left panel and Supplementary data 5B, respectively) and confirming by the absence of cleaved-PARP expression after BYL719 treatment in HOS osteosarcoma cells (Figure 1E, right panel). Similar data were obtained with MG-63, POS-1 (data not shown) and OSRGA cell lines (Supplementary data 4D). Migration assays were also performed on HOS and MOS-J cells to determine the effect of BYL719 on cell motility and demonstrated that BYL719 decreased cell motility (Supplementary data 6A and B). We then performed a recovery assay. Surprisingly, the treated cells are able to recovery in the same manner than in the control condition, suggesting that BYL719 as a cytostatic effect only when the drug is present (Figure 4C). All these data suggest that BYL719 has cytostatic activity in osteosarcoma cells.

BYL719 simultaneously reduces tumor growth and tumor ectopic bone formations in two murine models of osteosarcoma and slightly modulates systemic bone parameters

We next tested the effects of BYL719 in the murine MOS-J syngenic model of osteosarcoma. BYL719 significantly reduced tumor volumes in a dose-dependent manner compared to a vehicle group (Figure 2A; $p<0.01$ and $p<0.001$ respectively for 12.5 and 50 mg/kg BYL719). Indeed, the mean tumor volume decreased from 1747 mm^3 in the control group to 938 mm^3 for the group treated with 50 mg/kg BYL719 (Figure 2A, $p<0.001$). In addition, µCT analyses were performed on the tibias with the tumors and the contralateral tibias (normal bone) of each mouse. MicroCT analyses of the tibias bearing tumor showed the ectopic bone formation deposited by the tumor cells and clearly demonstrated that BYL719 significantly reduced this tumor ectopic bone (Figure 2B left panel). The benefit of BYL719 was confirmed with the calcified tissue parameters measured (Figure 2B, right panel). The bone volume (BV) was significantly decreased with 50 mg/kg BYL719, 7.08 ± 0.6 to 4.37 ± 0.21 mm^3 ($p<0.001$) as was the bone surface (BS) from 99.65 ± 5.74 mm^2 to 63.91 ± 2.3 mm^2 ($p<0.001$).

Histomorphometric parameters of contralateral tibias were studied to determine the systemic effect of BYL719 on normal bone remodeling without any tumor (Supplementary data 7). BYL719 at 50mg/kg/day did not affect any of the studied trabecular bone parameters (Supplementary data 7). However, it significantly reduced several cortical bone parameters including TV (Tissue Volume), BV, BV/TV, BS/TV and CTh ($p<0.01$) (Supplementary data 7). Histological investigations revealed that BYL719 decreased the surface of $TRAP^+$ osteoclasts without affecting the number of $osterix^+$ cells (Figures 3A, B). In addition, the therapeutic benefit of BYL719 was strengthened by the decrease of $KI67^+$ cell number (Figure 3C) and by a reduction of the tumor vascularization (Figure 3D).

Based on these results, the therapeutic potential of BYL719 was analyzed in a xenogenic model of osteosarcoma. Nude mice with human HOS tumors were treated with 50 mg/kg/day of BYL719. As with the MOS-J model, BYL719 significantly reduced tumor volumes, from 1445 mm^3 for the control group to 650 mm^3 for the treated group at the end of the treatment period (Figure 2C; $p<0.01$). These results confirmed the inhibitory effect of BYL719 in a second pre-clinical osteosarcoma model. MicroCT analysis of the tibias bearing tumor revealed that BYL719 reduced deposition of ectopic bone matrix as shown by the bone parameters values from 64.91 ± 5.2 to 36.4 ± 0.70 mm^2 ($p<0.001$) and from $6.2 \pm 0.33$to 4.0 ± 0.08 mm^3 ($p<0.001$) respectively for BS and BV (Figure 2D right panel). The effect of BYL719 on normal bone was evaluated by µCT of the contralateral tibia without any tumor confirming the results obtained in the syngenic MOS-J model (Supplementary data 8). MicroCT confirmed the effect of BYL719 on cortical bone observed in C57Bl5J mice.

Therapeutic benefit of combining BYL719 with conventional chemotherapeutic agents

As BYL719 shows a cytostatic effect in osteosarcoma cells, we then assessed the therapeutic benefit to combine BYL719 with ifosfamide (mafosfamide for *in vitro* experiment) a

conventional chemotherapy in the treatment of osteosarcoma. To determine whether this effect was additive or synergistic, the dose-dependent effects with constant ratio design and the combination index (CI) values were performed and calculated according to the Chou and Talalay median effect principal. Figures 4A and B show the dose response curve (combination treatment, BYL719 or mafosfamide monotherapy) and the combination index plots, indicating that BYL719 synergistically enhances the effect of mafosfamide on tumor cell growth (Figures 4A and B). Then we performed a colony formation assay to evaluate capabilities to recover after 2 days of BYL719 +/- mafosfamide treatment. While BYL719 did not change the number of colonies, mafosfamide decreased the colony formation compared with control (Figure 4C). However, the combination of BYL719 with mafosfamide significantly induced the highest decrease of colony formation compared with each single drug alone (Figure 4C). Moreover, BYL719 potentiates the effect of mafosfamide to induce apoptosis as shown by the increase of cleaved-PARP expression (Figure 4D).

We then studied the effect of BYL719 (50 mg/kg/day) combined with a sub-optimal dose of ifosfamide (IFOS, 30 mg/kg/day for 3 days) the syngenic murine model previously described (Figure 4E). As expected, 50 mg/kg BYL719 had a significantly inhibitory effect on tumor development compared to the control group. In contrast, combined treatment of a sub-optimal dose of IFOS with 50 mg/kg/day BYL719 significantly decreased tumor growth (1011 mm^3) compared to using IFOS alone (1746 mm^3) or BYL719 alone (1421 mm^3)(Figure 4E). MicroCT analysis of tumor bones revealed that the combined treatment did not have an impact on the therapeutic response of BYL719, not even synergistic or additive effects were observed on the ectopic bone formed (Figure 4F et G). These results strongly demonstrate the therapeutic interest to combine BYL719 with a conventional chemotherapeutic drug, in order to markedly delay tumor growth and tumor ectopic bone formation.

Osteoblast and osteoclast lineages are two targets of BYL719

To investigate the potential of BYL719 on osteoblast lineage, dose-response experiments were first assessed on hMSC viability by XTT assay. After 72 hours of treatment, BYL719 decreased hMSC viability with an IC_{50} of 8 µM (Figure 5A). In agreement with this effect, the mineralization process analyzed by alizarin red staining decreased in a dose-dependent manner as observed in Figure 5B. Osteoblast markers were then investigated by qRT-PCR (Figure 5C). BYL719 has a dual activity on osteoblast differentiation, characterized by an up-modulation of osteoblast markers in the early stages of culture time (*RUNX2* on D8 of the culture and ALP on D11 of the culture) and by a down-regulation of osteoblast markers such *ALP* at a later stage of the differentiation process (D21) when BYL719 was used at low doses (5 µM) (Figure 5C).

We next examined the effect of BYL719 on osteoclast differentiation *in vitro.* BYL719 decreased osteoclast numbers in a dose-dependent manner with full inhibition at 15 µM (Figure 6A). To determine whether this inhibition was due to the direct effect on osteoclast precursors and/or on mature osteoclasts by affecting cell viability, an XTT assay was performed on $CD14^+$ cells and on differentiated osteoclasts. BYL719 induced a marked inhibition of $CD14^+$ cell survival after 72 hours of treatment (Figure 6B) and also affected mature osteoclasts by decreasing their number by around 30 % compared to the control at 10 µM (Figure 6C). The effect of BYL719 on the expression of osteoclast markers and on their resorption capacity was then analyzed. As with the effects of BYL719 observed on osteoblast lineage, 5µM BYL719, which did not totally inhibit the differentiation of osteoclasts (Figure 6A), differentially regulated osteoclast markers. BYL719 decreased *NFATc1*and *MMP9* expression but increased *CATHK* and *TRAP* expression (Figure 6D) and weakly reduced the apparent capacity of osteoclast to resorb the calcified matrix (area resorbed in the determined regions of interest:

23.1% for the control compared to 14.5% in the presence of 5 μM of BYL719) (Figure 6E). Overall, these data reveal the dual effect of BYL719 on the differentiation of osteoblasts and osteoclasts.

DISCUSSION

Current treatment protocols for osteosarcoma are based on surgical resection associated with multiple highly toxic chemotherapy, the drugs used being adapted to the therapeutic response throughout the treatment period (3-5). Unfortunately, no therapeutic response is frequently observed with the establishment of lung metastases, which partly explains the survival rate. New therapeutic approaches are thus required and numerous clinical trials are ongoing to assess new drugs (7). Phosphatidylinositol-3-kinases (PI3K) have pleiotropic activities and then act as a key crossroad for numerous cell processes such as controlling cell proliferation, differentiation and death. Dysregulation of the PI3K/mTOR pathway, mainly due to redundant autocrine pathways rather than mutations, is clearly involved in the pathogenesis of sarcomas (37,38). Given their central role in cell biology, PI3K targeting is a therapeutic opportunity in medical oncology and has stimulated the development of selective inhibitors (7,14,33). Recently, we demonstrated that a dual mTOR/PI3K inhibitor, NVP-BEZ235, shows a therapeutic interest and may be considered as an adjuvant drug for bone sarcomas (39). In this context, the present work demonstrates the potential therapeutic value of BYL719 for osteosarcoma.

BYL719 has a cytostatic effect, and inhibits cell proliferation by inducing a cell cycle blockade in the G0/G1 phase in the absence of cell death. Consequently, BYL719 slows down tumor growth in pre-clinical models of osteosarcoma by affecting cell proliferation, tumor vascularization and bone cell differentiation. Interestingly, combining BYL719 with conventional chemotherapy shows additive effects on tumor growth. In addition, osteoblasts

and osteoclasts can be also potential targets of BYL719. Given these data, BYL719 appears to have several cellular targets in osteosarcoma and may exert its activity through direct (cancer cells) or indirect effects by acting on the tumor microenvironment. Of the components of this microenvironment, endothelial cells that deliver the drug to the tumor are affected by BYL719 as shown by the lower number of $CD146^+$ and $CD31^+$ cells after BYL719 inoculation. It is well admitted that blood vessels play a strategic role in tumorigenesis by delivering nutrients and oxygen (40). In addition, by responding to diverse environmental alterations, PI3K is involved in the angiogenic process by regulating vascular growth and maintenance (41). Several studies have demonstrated that increased tumor vascularity is associated with a poor prognosis in osteosarcoma and correlated with tumor progression, especially metastases formation (6, 42-45). Combination of BYL719 with conventional chemotherapy showed a promising therapeutic improvement and underlines the value of multidrug approaches for bone sarcomas (3, 7, 20, 46).

Similarly to metastatic carcinoma to bone, a vicious cycle between osteoclasts, bone stromal cells/osteoblasts, and cancer cells has been hypothesized during the development of osteosarcoma (47). Accordingly, targeting osteoclasts or inhibiting osteoclast activity has been shown to have significant efficacy in inhibiting local cancer growth (36, 46, 47). Like specific anti-resorptive agents (bisphosphonates, osteoprotegerin, etc), BYL719 inhibits the number of $TRAP^+$ osteoclasts in pre-clinical models of osteosarcoma. This effect is in agreement with the role of PI3K in osteoclastogenesis (formation of ruffled borders, vesicular transport, cellular trafficking, etc) (48). However, this observation is partly in accordance to the *in vitro* experiments in which BYL719 exerts differential effects depending on the doses used with a significant inhibition of osteoclastogenesis at high doses, as well as an increase of several osteoclast markers and a slight inhibition of bone resorption. The harmful effects of BYL719 are explained by its cytotoxic activity on osteoclast precursors and its modest effect on viability

of mature osteoclasts in concordance with the role of PI3K in osteoclasts. Similarly, osteoblast differentiation was also affected by BYL719 treatment and, whereas high doses of BYL719 diminished osteoblast proliferation, and mineralization, low doses stimulated osteoblastic markers at an early stage in the culture time and down-regulated osteoblast markers such *ALP* at a later stage of the differentiation. Such dual effects have been already observed with chemical inhibitors of the tyrosine kinase receptor mediating PI3K signaling. Imatinib mesylate (Gleevec), for example, inhibits osteoblast proliferation and activates their activities in particular through its inhibitory activity on PDGFRβ (49). MicroCT experiments suggest more complex activities for BYL719 on bone cells. If trabecular bone is not affected by the drug in C57Bl/6J, BYL719 has a catabolic effect on nude mice, suggesting a potential compensatory effect of BYL719 on bone tissue via immune cells. This hypothesis is strengthened by the fact that nude mice exhibited hyperglycemia not observed in immunocompetent mice (data not shown). In addition, the absence of variation of global trabecular bone parameters is associated with a marked decrease in $TRAP^+$ cell numbers and no alteration in osteoblast numbers. Such mechanisms may be explained by the individual increase in resorptive activity of the viable osteoclasts and/or bone forming activity of osteoblasts. MicroCT also revealed that in the absence of marked modulation of trabecular bone, BYL719 decreased in particular cortical thickness in both models used. The dual activity will require additional experiments to better understand its effect on the balance between osteoblast and osteoclast functions with a specific focus on immune cells.

Clinical investigations using BYL719 started in 2010 exclusively in patients with advanced solid tumors with *PIK3CA* mutations. The preliminary safety report shows that BYL719 is well tolerated (maximal doses studied: 400 mg/d). The first signs of clinical efficacy have been evidenced in a patient with breast carcinoma treated at 270 mg/d (24) .The safety profile of BYL719 is characterized by on-target toxicity including hyperglycemia

especially at high doses which is reversible with drug interruption, nausea, decreased appetite, diarrhea and vomiting. *In fine*, BYL719 appears to induce manageable side effects, compared to LY294002 and Wortmannin that never progressed into clinical trials because of liver and skin cytotoxicity (50).

Overall, our data provide the first evidence for using BYL719, a new α-specific PI3K inhibitor, to improve the therapeutic outcome of osteosarcoma patients. Its combination with conventional chemotherapeutic drugs in the treatment of sarcoma patients may be envisaged. The significance of this combination now opens new eras in the field of multidrug strategies for the treatment of bone sarcomas, especially in osteosarcoma.

Acknowledgements:

Bérengère Gobin received a PhD fellowship from the Region des Pays de la Loire and INSERM. We thank Martine Berreur for her technical help for measuring the resorption activity of osteoclasts.

REFERENCES

1. Picci P. Osteosarcoma (osteogenic sarcoma). *Orphanet J Rare Dis* 2007;**2**:6.

2. Hauben EI, Hogendoorn PCW. Epidemiology of primary bone tumors and economical aspects of bone metastases. In: Heymann D, editor. Bone Caner: progression and therapeutic approaches. Academic Press (Elsevier); 2010. 504p.

3. Heymann D, Rédini F. Bone sarcomas: pathogenesis and new therapeutic approaches. *IBMS BoneKEy* 2011;**8**:402-14.

4. Ando K, Heymann MF, Stresing V, Mori K, Redini F, Heymann D. Current therapeutic strategy and novel approaches in osteosarcoma. *Cancers* 2013;**5**: 591-616.

5. Hattinger CM, Pasello M, Ferrari S, Picci P, Serra M. Emerging drugs for high-grade osteosarcoma. *Expert Opin Emerg Drugs* 2010;**15**:615-34.

6. Ando K, Mori K, Verrecchia F, Baud'huin M, Rédini F, Heymann D. Molecular alterations associated with osteosarcoma Development. *Sarcoma* 2012:**523432**.

7. HeymannD, Rédini F. Targeted therapies for bone sarcomas. *BoneKey Reports* 2013; **112**.

8. Katso R, Okkenhaug K, Ahmadi K, White S, Timms J, Waterfield MD. Cellular function of phosphoinositide 3-kinases: implications for development, homeostasis, and cancer. *Annu Rev Cell Dev Biol* 2001;**17**:615-75.

9. Vanhaesebroeck B, Guillermet-Guibert J, Graupera M, Bilanges B. The emerging mechanisms of isoform-specific PI3K signalling. *Nat Rev Mol Cell Biol* 2010;**11**:329-41.

10. Sopasakis VR, Liu P, Suzuki R, Kondo T, Winnay J, Tran TT, Asano T, Smyth G, Sajan MP, Farese RV, Kahn CR *et al.* Specific roles of the p110 alpha isoform of phosphatidylinsositol 3-kinase in hepatic insulin signaling and metabolic regulation. *Cell Metabol* 2010; **11**:220-30

11. Smith GC, Ong WK, Rewcastle GW, Kendall JD, Han W, Shepherd PR. Effects of acutely inhibiting PI3K isoforms and mTOR on regulation of glucose metabolism *in vivo*. *Biochem J* 2012;**442**:161-9.
12. Vadas O, Burke JE, Zhang X, Berndt A, Williams RL. Structural basis for activation and inhibition of class I phosphoinositide 3-kinases. *Sci Signal* 2011;**4**:re2.
13. Janku F, Wheler JJ, Naing A, Stepanek VM, Falchook GS, Fu S, Garrido-Laguna I, Tsimberidou AM, Piha-Paul SA, Moulder SL, Lee JJ, Luthra R *et al*. PIK3CA mutations in advanced cancers: characteristics and outcomes. *Oncotarget* 2012;**3**:1566-75.
14. Brana I, Siu LL. Clinical development of phosphatidylinositol 3-kinase inhibitors for cancer treatment. *BMC Med* 2012;**10**:161.
15. Fallica B, Maffei JS, Villa S, Makin G, Zaman M. Alteration of cellular behavior and response to PI3K pathway inhibition by culture in 3D collagen gels. *PLoS One* 2012;**7**:e48024.
16. Zhao G, Cai C, Yang T, Qiu X, Liao B, Li W, Ji Z, Zhao J, Zhao H, Guo M, Ma Q, Xiao C *et al*. MicroRNA-221 induces cell survival and cisplatin resistance through PI3K/Akt pathway in human osteosarcoma. *PLoS One* 2013;**8**:e53906.
17. Wang K, Zhuang Y, Liu C, Li Y. Inhibition of c-Met activation sensitizes osteosarcoma cells to cisplatin via suppression of the PI3K-Akt signaling. *Arch Biochem Biophys* 2012;**526**:38-43.
18. Tsubaki M, Satou T, Itoh T, Imano M, Ogaki M, YanaeM, Nishida S. Reduction of metastasis, cell invasion, and adhesion in mouse osteosarcoma by YM529/ONO-5920-induced blockade of the Ras/MEK/ERK and Ras/PI3K/Akt pathway. *Toxicol Appl Pharmacol* 2012;**259**:402-10.

19. Fukaya Y, Ishiguro N, Senga T, Ichigotani Y, Sohara Y, Tsutsui M, Shioura T, Iwamoto T, Hamaguchi M. A role for PI3K-Akt signaling in pulmonary metastatic nodule formation of the osteosarcoma cell line, LM8. *Oncol Rep* 2005;**14**:847-52.
20. Moriceau G, Ory B, Mitrofan L, Riganti C, Blanchard F, Brion R, Charrier C, Battaglia S, Pilet P, Denis MG, Shultz LD, Mönkkönen J *et al*. Zoledronic acid potentiates mTOR inhibition and abolishes the resistance of osteosarcoma cells to RAD001 (Everolimus): pivotal role of the prenylation process. *Cancer Res* 2010;**70**:10329-39.
21. Choy E, Hornicek F, MacConaill L, Harmon D, Tariq Z, Garraway L, Duan Z. High-throughput genotyping in osteosarcoma identifies multiple mutations in phosphoinositide-3-kinase and other oncogenes. *Cancer* 2012;**118**:2905-14.
22. Furet P, Guagnano V, Fairhurst RA, Imbach-Weese P, Bruce I, Knapp M, Fritsch C, Blasco F, Blanz J, Aichholz R, Hamon J, Fabbro D *et al.* Discovery of NVP-BYL719 a potent and selective phosphatidylinositol-3 kinase alpha inhibitor selected for clinical evaluation. *Bioorg Med Chem Lett* 2013;**23**:3741-8.
23. Juric D, Rodon J, Gonzalez-Angulo AM, Burris HA, Bendell J, Berlin JD, Middleton MR, Bootle D, Boehm M, Schmitt A, Rouyrre N, Quadt C *et al*. BYL719, a next generation PI3K alpha specific inhibitor: Preliminary safety, PK, and efficacy results from the first-in-human study. *Cancer Res* 2012;**72**:Supp1.
24. Juric D, Argiles G, Burris HA, Gonzalez-Angulo AM, Saura C, Quadt C, Douglas M, Demanse D, De Buck S, Baselga J. Phase I study of BYL719, an alpha-specific PI3K inhibitor in patients with PIK3CA mutant advanced solid tumors: preliminary efficacy and safety in patients with PIK3CA mutant ER-positive (ER+) metastatic breast cancer (MBC). *Cancer Res* 2012;**73**:Supp 1.

25. Klein B, Pals S, Masse R, Lafuma J, Morin M, Binart N, Jasmin JR, Jasmin C. Studies of bone and soft-tissue tumours induced in rats with radioactive cerium chloride. *Int J Cancer* 1977;**20**:112-19.
26. Thiery J, Perdereau B, Gongora R, Gongora C, Mazabraud A. Un modele experimental d'osteosarcome chez le rat. *Sem Hop Paris* 1982;**58**:1686-89.
27. Kamijo A, Koshino T, Uesugi M, Nitto H, Saito T. Inhibition of lung metastasis of osteosarcoma cell line POS-1 transplanted into mice by thigh ligation. *Cancer Lett* 2002; **188**:213-19.
28. Joliat MJ, Umeda S, Lyons BL, Lynes MA, Shultz LD. Establishment and characterization of a new osteogenic cell line (MOS-J) from a spontaneous C57BL/6J mouse osteosarcoma. *In Vivo* 2002;**16**:223– 8.
29. Bouacida A, Rosset P, Trichet V, Guilloton F, Espagnolle N, Cordonier T, Heymann D, Layrolle P, Sensébé L, Deschaseaux F. Pericyte-like progenitors show high immaturity and engraftment potential as compared with mesenchymal stem cells. *PLoS One* 2012;**7**:e48648
30. Guihard P, Danger Y, Brounais B, David E, Brion R, Delecrin J, Richards CD, Chevalier S, Rédini F, Heymann D, Gascan H, Blanchard F. Induction of osteogenesis in mesenchymal stem cells by activated monocytes/macrophages depends on oncostatin M signaling. *Stem Cells* 2012;**30**:762-72.
31. Bohic S, Pilet P, Heymann D. Effects of leukemia inhibitory factor and oncostatin M on bone mineral formed in in vitro rat bone-marrow stromal cell culture: physicochemical aspects. *Biochem Biophys Res Commun*1998;**253**:506-13.
32. Baud'huin M, Renault R, Charrier C, Riet A, Moreau A, Brion R, Gouin F, Duplomb L, Heymann D. Interleukin-34 is expressed by giant cell tumours of bone and plays a key role in RANKL-induced osteoclastogenesis. *J Pathol* 2010;**221**:77-86.

33. Baud'huin M, Charrier C, Bougras G, Brion R, Lezot F, Padrines M, Heymann D. Proteoglycans and osteolysis. *Methods Mol Biol* 2012;**836**:323-37.
34. Vandesompele J, De Preter K, Pattyn F, Poppe B, Van Roy N, De Paepe A, Speleman F. Accurate normalization of real-time quantitative RT-PCR data by geometric averaging of multiple internal control genes. *Genome Biol* 2002;**3**:RESEARCH0034.
35. Pfaffl MW. A new mathematical model for relative quantification in real-time RT-PCR. *Nucleic Acid Res* 2001;**29**:e45.
36. Lamoureux F, Richard P, Wittrant Y, Battaglia S, Pilet P, Trichet V, Blanchard F, Gouin F, Pitard B, Heymann D, Redini F. Therapeutic relevance of osteoprotegerin gene therapy in osteosarcoma: blockade of the vicious cycle between tumor cell proliferation and bone resorption. *Cancer Res* 2007;**67**:7308-18.
37. Mahalingam D, Mita A, Sankhala K, Swords R, Kelly K, Giles F, Mita MM. Targeting sarcomas: novel biological agents and future perspectives. *Curr Drug Targets* 2009;**10**:937-49.
38. Blay JY. Updating progress in sarcoma therapy with mTOR inhibitors. *Ann Oncol* 2011; **22**:280-7.
39. Gobin B, Battaglia S, Lanel R, Chesneau J, Amiaud J, Redini F, Ory B, Heymann D. NVP-BEZ235, a dual PI3K/mTOR inhibitor, inhibits osteosarcoma cell proliferation and tumor development *in vivo* with an improved survival rate. *Cancer Lett* 2014;**344** :291-298.
40. Fokas E, McKenna WG, Muschel RJ. The impact of tumor microenvironment on cancer treatment and its modulation by direct and indirect antivascular strategies. *Cancer Metastasis Rev* 2012;**31**:823-42.
41. Graupera M, Potente M. Regulation of angiogenesis by PI3K signaling networks. *Exp Cell Res* 2013;**319**:1348-55.

42. Lee YH, Tokunaga T, Oshika Y, Suto R, Yanagisawa K, Tomisawa M, Fukuda H, Nakano H, Abe S, Tateishi A, Kijima H, Yamazaki H *et al*. Cell-retained isoforms of vascular endothelial growth factor (VEGF) are correlated with poorprognosis in osteosarcoma. *Eur J Cancer* 1999;**35**:1089-93.

43. Kaya M, Wada T, Akatsuka T, Kawaguchi S, Nagoya S, Shindoh M, Higashino F, Mezawa F, Okada F, Ishii S. Vascular endothelial growth factor expression in untreated osteosarcoma is predictive of pulmonary metastasis and poor prognosis. *Clin Cancer Res* 2000;**6**:572-7.

44. Abdeen A, Chou AJ, Healey JH, Khanna C, Osborne TS, Hewitt SM, Kim M, Wang D, Moody K, Gorlick R. Correlation between clinical outcome and growth factor pathway expression in osteogenic sarcoma. *Cancer* 2009;**115**:5243-50.

45. Kreuter M, Bieker R, Bielack SS, Auras T, Buerger H, Gosheger G, Jurgens H, Berdel WE, Mesters RM. Prognostic relevance of increased angiogenesis in osteosarcoma. Clin Cancer Res 2004;**10**:8531-7.

46. Wittrant Y, Théoleyre S, Chipoy C, Padrines M, Blanchard F, Heymann D, Redini F.RANKL/RANK/OPG: new therapeutic targets in bone tumours and associated osteolysis. *Biochim Biophys Acta* 2004;**20**:1704:49-57.

47. Moriceau G, Ory B, Gobin B, Verrecchia F, Gouin F, Blanchard F, Redini F, Heymann D. Therapeutic approach of primary bone tumours by bisphosphonates. *Curr Pharm Des* 2010;**16**:2981–87.

48. Shinohara M, Nakamura M, Masuda H, Hirose J, Kadono Y, Iwasawa M, Nagase Y, Ueki K, Kadowaki T, Sasaki T, Kato S, Nakamura H *et al*. Class IA phosphatidylinositol 3-kinase regulates osteoclastic bone resorption through protein kinaseB-mediated vesicle trasnport *J Bone Miner Res* 2012;**27**:2464-75.

49. Vandyke K, Fitter S, Dewar AL, Hughes TP, Zannettino ACW. Dysregulation of bone remodeling by imatinib mesylate. *Blood* 2010;**115**:766-74.
50. Dan S, Okamura M, Seki M, Yamazaki K, Sugita H, Okui M, Mukai Y, Nishimura H, Asaka R, Nomura K, Ishikawa Y, Yamori T. Correlating phosphatidylinositol 3-kinase inhibitor efficacy with signaling pathway status: in silico and biological evaluations. *Cancer Res* 2010;**70**:4982-94.

FIGURE LEGENDS

Figure 1: BYL719 decreases cell growth but failed to induce in human (MG-63, HOS) and murine (MOS-J, POS-1) osteosarcoma cells. (**A**) Chemical structure of BYL719. (**B**) Analysis of PI3K pathway after a time course experiment of BYL719 (25 µM) on HOS and MOS-J cells. (**C**) Viability assay on human and murine cells after 72 hours of treatment with increasing doses of BYL719. IC_{50} and IC_{90} for osteosarcoma cell lines are reported in the table. (**D**) Manual cell counting of both alive (grey) and dead cells (black) after 24 and 48 hours of treatment with BYL719 at indicated doses in HOS cells. (**E**) Caspase 3/7 activity assay in a time course experiment with 25 µM BYL719 in HOS cells. STS (Staurosporin) was used as positive control of caspase 3/7 activity (*left panel*). HOS cells were treated with BYL719 at indicated doses, and apoptosis was evaluated by cleaved ploy (ADP-ribose) polymerase (PARP) level by western blotting (*right panel*). Data are presented as the percentage of untreated control cells and are expressed as the mean ± SD of 3 independent experiments. * P <0.05; ***, P <0.001 compared to the control.

Figure 2: BYL719 inhibits tumor growth in pre-clinical murine models of osteosarcoma. C57Bl/6J with MOS-J tumors (n=6 per group) were randomized as controls (vehicle) or BYL719 (12.5 mg/kg/day or 50 mg/kg/day) (**A, B**) and nude mice with HOS-MNNG tumors (n=8 per group) were randomized as controls (vehicle) or BYL719 50 mg/kg/day (**C, D)**. The preventive treatment started 1 day after tumor cell implantation. The mean tumor volume was followed twice a week (**A, C**). Representative µCT images of the ectopic bone (red) of tibias with tumors, taken *ex vivo*, from treated mice with MOS-J (**B left panel**) or from mice with HOS-MNNG (**C left panel**) treated with BYL719 (50 mg/kg/day) or vehicle (Control). MicroCT analysis of the ectopic bone [BS (mm^2), BV (mm^3)] from treated mice bearing MOS-

J tumors (**B right panel**) or from mice bearing HOS-MNNG tumors (**C right panel**) treated with the vehicle (CT) or BYL719 (50 mg/kg/day). * P <0.05; ** P <0.01; *** P < 0.001.

Figure 3: BYL719 inhibits osteoclast numbers, osteosarcoma cell proliferation and reduces tumor vascularization *in vivo*. C57Bl/6J with MOS-J tumors (n=6 per group) were assigned as controls (vehicle), or BYL719 (50 mg/kg/day). Osterix (**A**) and TRAP (**B**) were evaluated by means of immunohistochemical and histoenzymatic analysis respectively on the limb with no tumor. Specimens were scored and estimated in terms of the number of positive cells +/- SD for osterix, and the surface occupied by osteoclasts was determined by Image J in the delimited ROI. $KI67^{+}$ cells in the tumor mass were scored by means of immunohistochemistry and estimated in terms of the number of positive cells +/- SD in the delimited ROI (**C**). Tumor vascularization was studied by following the positive expression of CD31 and CD146 using immunohistochemistry **(D)**. NS: not significant; ** P <0.01; *** P < 0.001.

Figure 4: BYL719 synergistically enhances effects of chemotherapy to delay tumor growth of osteosarcoma cells *both in vitro* and *in vivo*. (**A**) MOS-J osteosarcoma cells were treated with BYL719 followed by mafosfamide at the indicated doses for 48 hours. Cell growth was determined by crystal violet and compared with control. (B) Dose-dependent effects and CI values calculated by CalcuSyn software were assessed in osteosarcoma cells treated for 48 hours with BYL719 alone, mafosfamide alone, or combined treatement at indicated doses with constant ratio design between both drugs (*left panel*). The CI for ED_{50}, ED_{75} and ED_{90} were lower than 1, indicative of a synergistic effect of this combined treatment (*right panel*). (C) Osteosarcoma cells were treated with 25µM BYL719 +/- 12.5µg/ml mafosfamide for 2 days,

and then plated at clonal density for colony counts after crystal violet staining. (D) Osteosarcoma cells were treated with 25µM BYL719 +/- 12.5µg/ml mafosfamide for 2 days. Cells were harvested, and apoptosis was evaluated by cleaved-PARP level by western blotting. (E) Summary of the experimental protocol. C57Bl/6J with MOS-J tumors (n=8 per group) were randomized in control (vehicle), BYL719 (50 mg/kg/day), IFOS (30mg/kg/day on 5, 6 and 7 after cell implantation) or BYL719 combined with IFOS groups. The mean tumor volumes were measured twice a week. (**F**) Representative images of the ectopic bone (red) of tibias with tumors, taken *ex vivo*, from mice with MOS-J treated with IFOS, BYL719, BYL719+IFOS or the vehicle (Control). (G) MicroCT analysis of the ectopic bone [BS (mm^2), BV (mm^3)] from mice bearing MOS-J tumor. * P <0.05; ** P <0.01; *** P < 0.001.

Figure 5: BYL719 modulates osteoblast differentiation and activity. (A) Human MSCs were treated with increasing doses of BYL719 for 72h and cell viability was measured by means of a colorimetric XTT assay. (**B**) hMSCs were cultured for 21 days in proliferation (CT-) or osteogenic differentiation medium (CT+) with or without BYL719. The mineralization capacity of hMSCs was determined by alizarin red staining. (**C**)Expression of *RUNX2* and *ALP* mRNA levels was assessed by qRT-PCR.

Figure 6: BYL719 inhibits osteoclast differentiation but not their resorptive capacity. (**A**) Multinucleated $TRAP^+$ cells, originated from $CD14^+$ cells, with more than three nuclei were considered to be osteoclasts and were counted manually (original magnification, ×400). (**B**) cell viability of $CD14^+$cells cultured with hRANKL (100ng/ml), hM-CSF (25ng/mL) or BYL719 (1-20 µM) for 72h was measured by means of a colorimetric XTT assay. (**C**) Differentiated osteoclasts were cultured without RANKL and hM-CSF but with BYL719 for 72h. Viable

TRAP$^+$ osteoclasts were counted manually. * $p<0.05$, ** $p<0.01$ compared to the control**.** (**D**) Expression of *NFATc1, MMP-9, CATHK*, and *TRAP* mRNA levels was assessed using quantitative RT-PCR. (**E**) CD14$^+$ cells were differentiated into osteoclasts on dentine slices with or without 5μM BYL719 for 11 days. Resorption pits on dentine slices were observed by scanning electron microscopy. CD14$^+$ cells cultured with hM-CSF and without RANKL were used as the negative control (control-). Representative images of pit formation on the dentine slices from two independent experiments are shown.

Figure 1

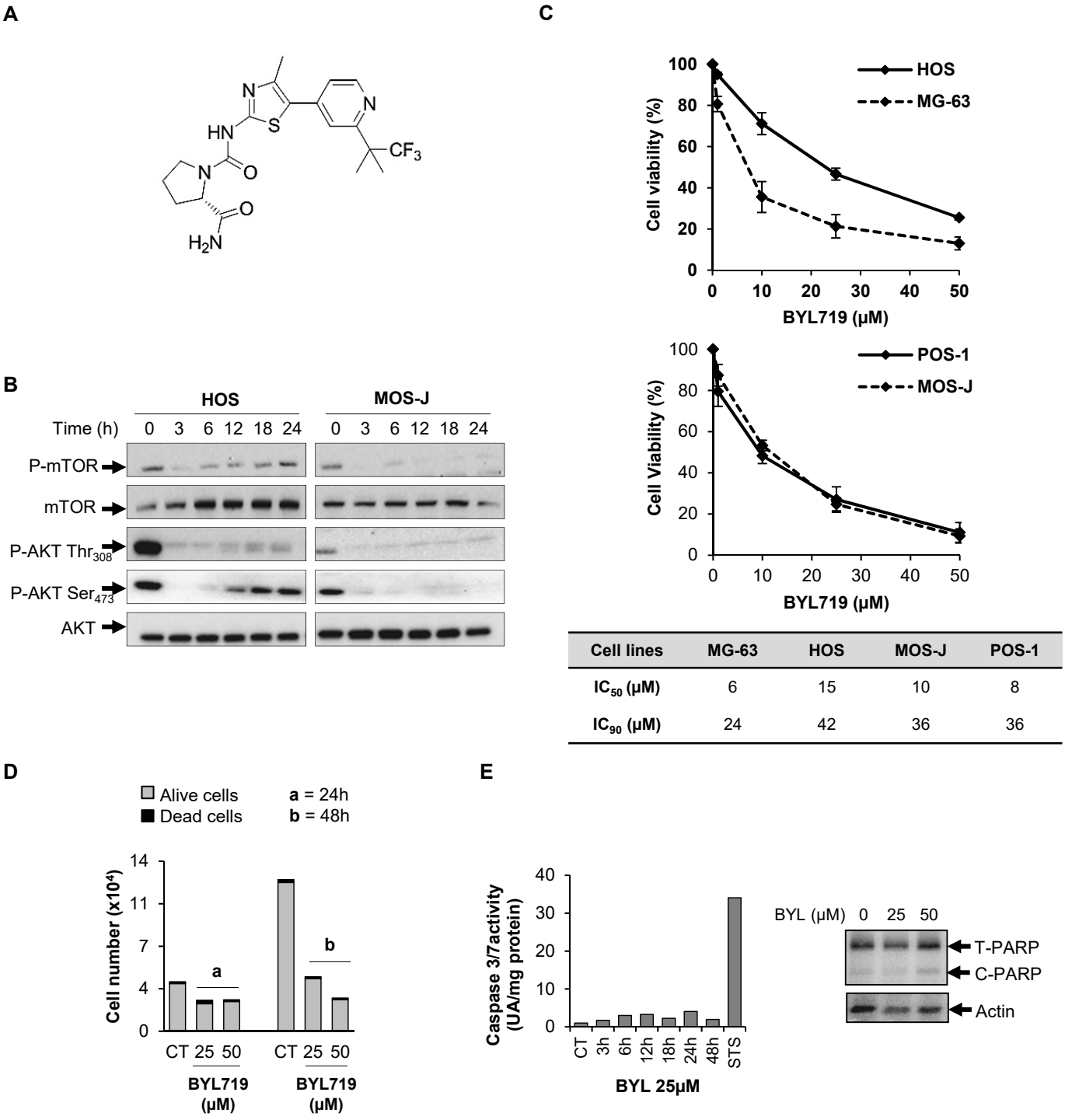

Cell lines	MG-63	HOS	MOS-J	POS-1
IC_{50} (µM)	6	15	10	8
IC_{90} (µM)	24	42	36	36

Figure 2

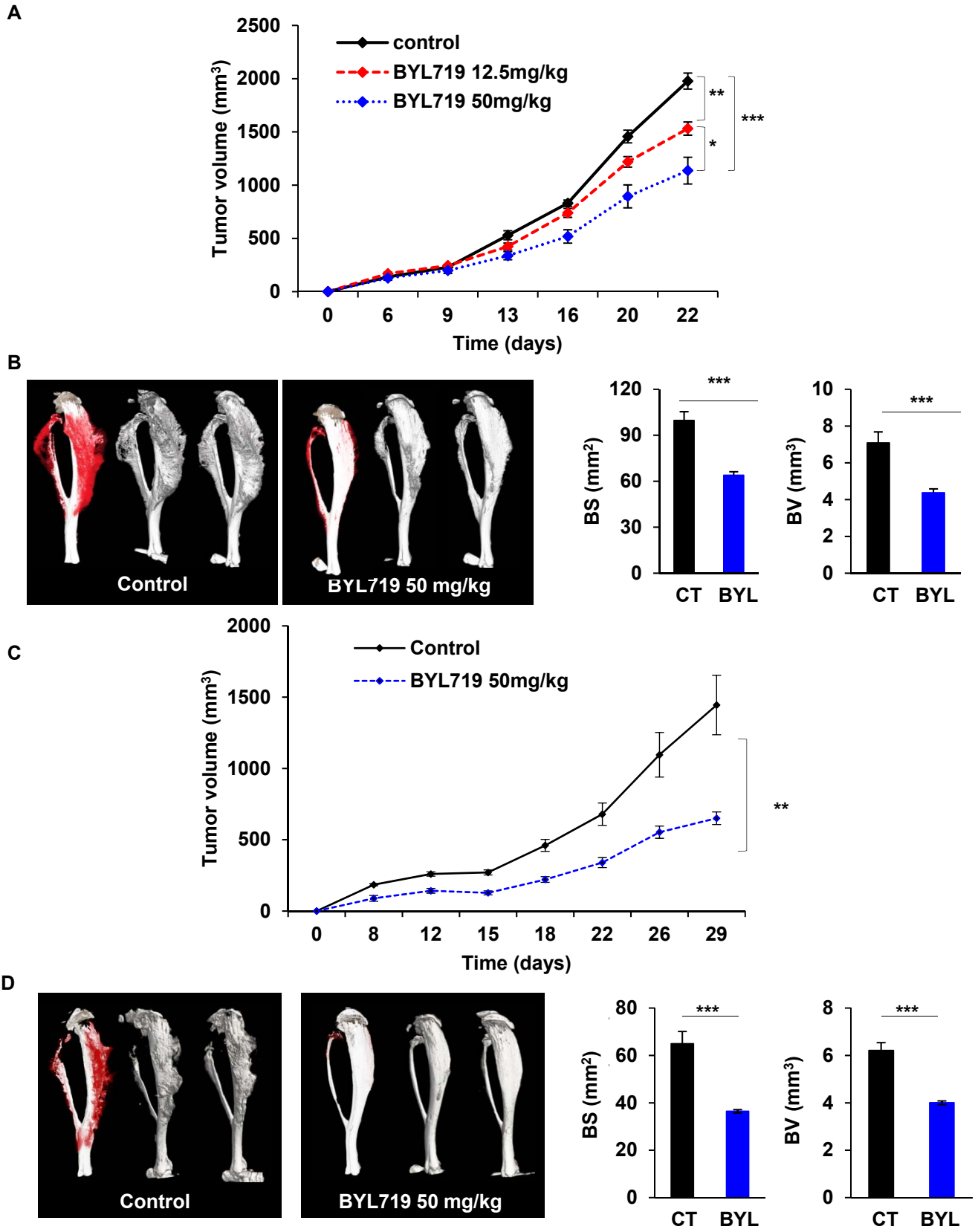
A
Tumor volume (mm³)
2500
2000
1500
1000
500
0
control
BYL719 12.5mg/kg
BYL719 50mg/kg
**
*
***
0
6
9
13
16
20
22
Time (days)
B
Control
BYL719 50 mg/kg
BS (mm²)
120
90
60
30
0
***
CT
BYL
BV (mm³)
10
8
6
4
2
0
***
CT
BYL
C
Tumor volume (mm³)
2000
1500
1000
500
0
Control
BYL719 50mg/kg
**
0
8
12
15
18
22
26
29
Time (days)
D
Control
BYL719 50 mg/kg
BS (mm²)
80
60
40
20
0
***
CT
BYL
BV (mm³)
8
6
4
2
0
***
CT
BYL

Figure 3

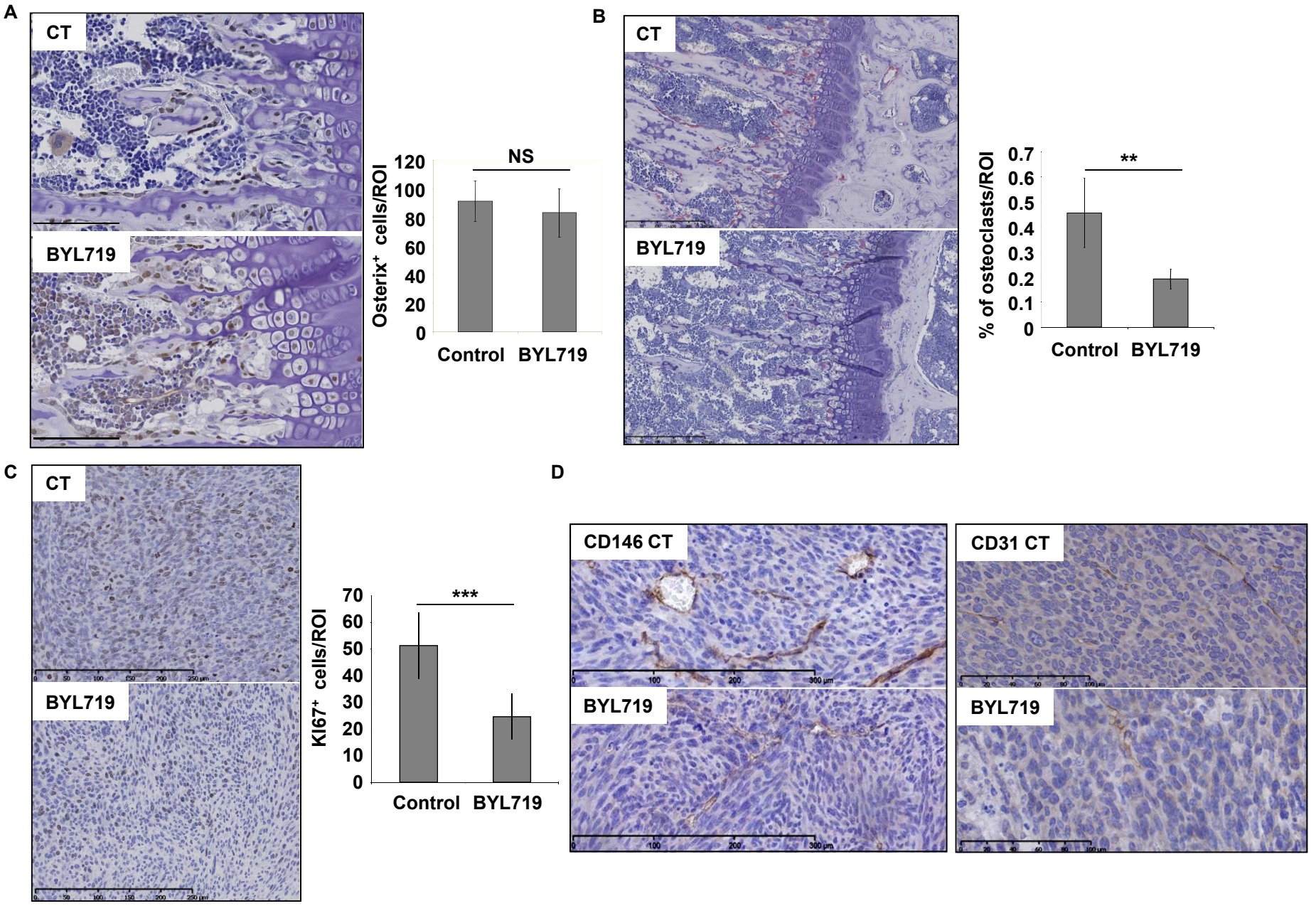
A
CT
BYL719
Osterix+ cells/ROI
120
100
80
60
40
20
0
NS
Control
BYL719
B
CT
BYL719
% of osteoclasts/ROI
0.7
0.6
0.5
0.4
0.3
0.2
0.1
0
**
Control
BYL719
C
CT
BYL719
KI67+ cells/ROI
70
60
50
40
30
20
10
0
***
Control
BYL719
D
CD146 CT
BYL719
CD31 CT
BYL719

Figure 4

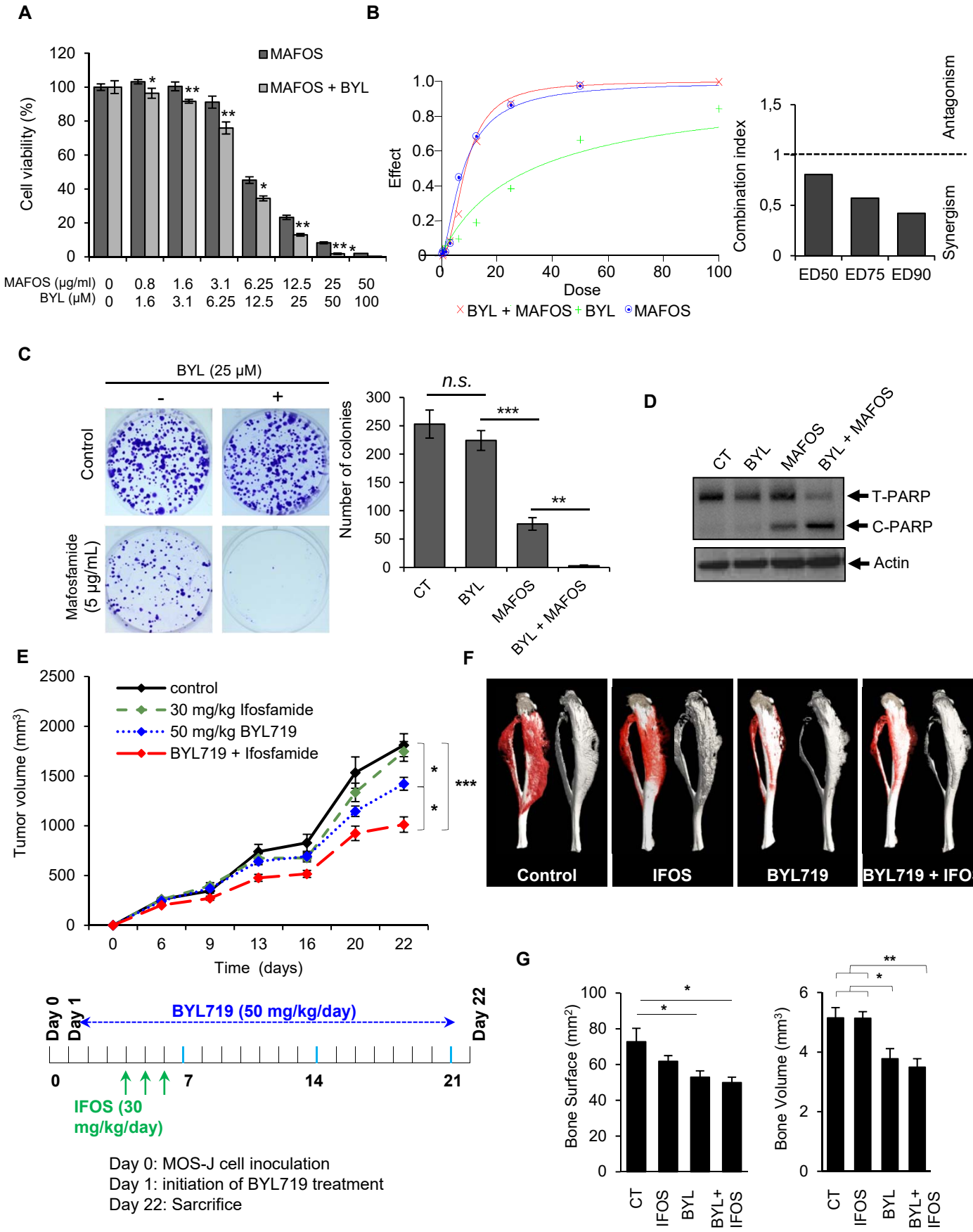

Day 0: MOS-J cell inoculation
Day 1: initiation of BYL719 treatment
Day 22: Sarcrifice

Figure 5

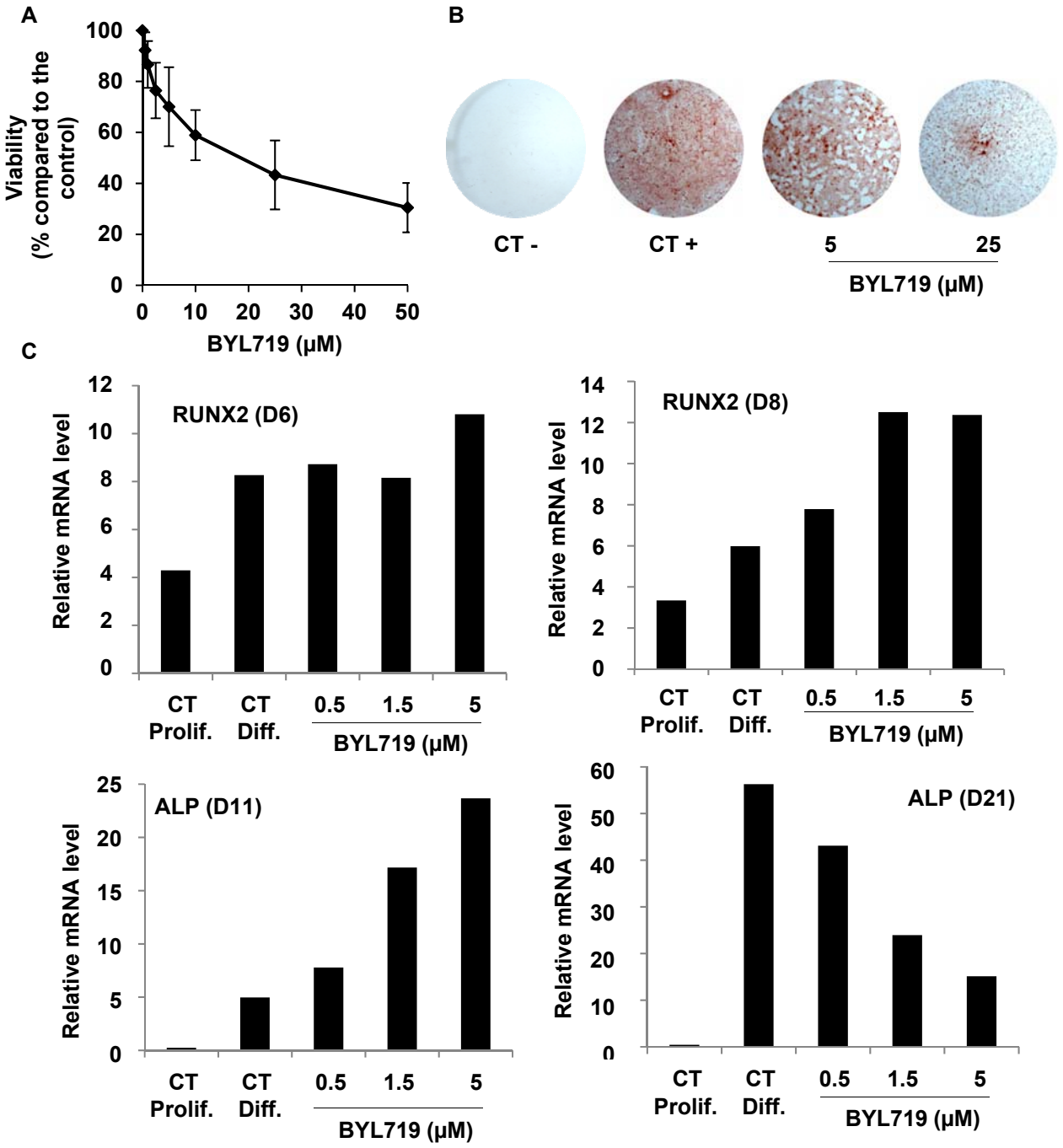
A
Viability (% compared to the control)
100
80
60
40
20
0
0
10
20
30
40
50
BYL719 (µM)
B
CT -
CT +
5
25
BYL719 (µM)
C
RUNX2 (D6)
Relative mRNA level
12
10
8
6
4
2
0
CT Prolif.
CT Diff.
0.5
1.5
5
BYL719 (µM)
RUNX2 (D8)
Relative mRNA level
14
12
10
8
6
4
2
0
CT Prolif.
CT Diff.
0.5
1.5
5
BYL719 (µM)
ALP (D11)
Relative mRNA level
25
20
15
10
5
0
CT Prolif.
CT Diff.
0.5
1.5
5
BYL719 (µM)
ALP (D21)
Relative mRNA level
60
50
40
30
20
10
0
CT Prolif.
CT Diff.
0.5
1.5
5
BYL719 (µM)

Figure 6

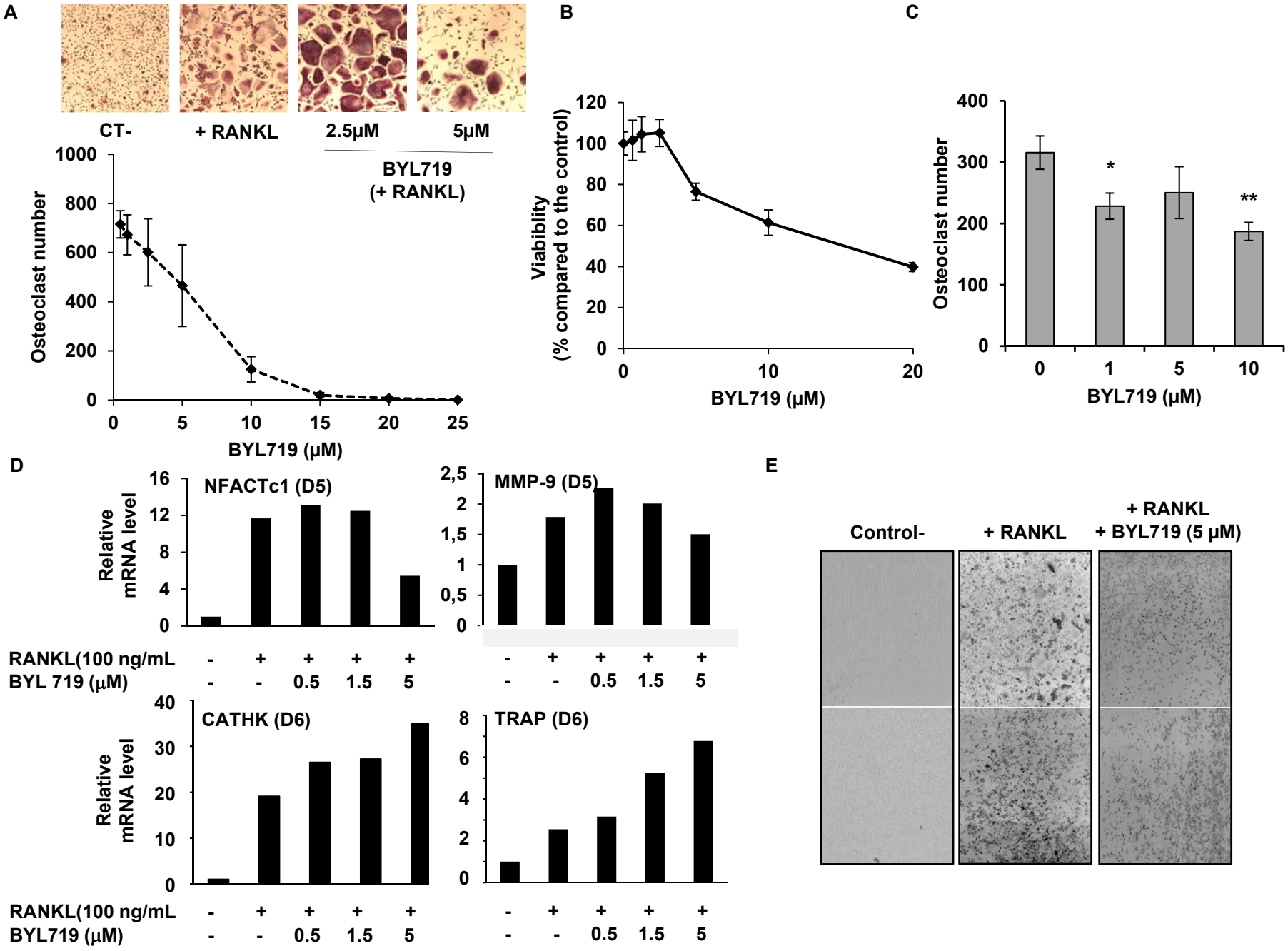
A
CT-
+ RANKL
2.5µM
5µM
BYL719
(+ RANKL)
Osteoclast number
BYL719 (µM)
B
Viability
(% compared to the control)
BYL719 (µM)
C
Osteoclast number
BYL719 (µM)
D
NFACTc1 (D5)
MMP-9 (D5)
CATHK (D6)
TRAP (D6)
Relative mRNA level
RANKL(100 ng/mL
BYL 719 (µM)
E
Control-
+ RANKL
+ RANKL
+ BYL719 (5 µM)